

Available online at www.sciencedirect.com**ScienceDirect**Journal homepage: www.elsevier.com/locate/cortex**Special issue: Research report**

Implicit attention to negative social, in contrast to nonsocial, words in the Stroop task differs between individuals high and low in loneliness: Evidence from event-related brain microstates

Stephanie Cacioppo ^{a,b,*}, Stephen Balogh ^b and John T. Cacioppo ^{a,b,c}

^a Department of Psychiatry and Behavioral Neuroscience, The University of Chicago Pritzker School of Medicine, USA

^b HPEN Laboratory, Center for Cognitive and Social Neuroscience, The University of Chicago, USA

^c Center for Cognitive and Social Neuroscience, The University of Chicago, USA

ARTICLE INFO**Article history:**

Received 30 November 2014

Reviewed 26 January 2015

Revised 22 April 2015

Accepted 27 May 2015

Published online 2 July 2015

ABSTRACT

Being on the social perimeter is not only sad, it is dangerous. Our evolutionary model of the effects of perceived social isolation (loneliness) on the brain as well as a growing body of behavioral research suggests that loneliness promotes short-term self-preservation, including an increased implicit vigilance for social, in contrast to nonsocial, threats. However, this hypothesis has not been tested previously in a neuroimaging study. We therefore used high density EEG and a social Stroop interference task to test the hypothesis that implicit attention to negative social, in contrast to nonsocial, Words in the Stroop task differs between individuals high versus low in loneliness and to investigate the brain dynamics of implicit processing for negative social (*vs* nonsocial) stimuli in lonely individuals, compared to nonlonely individuals ($N = 70$). The present study provides the first evidence that negative social stimuli are differentiated from negative nonsocial stimuli more quickly in the lonely than nonlonely brains. Given the timing of this differentiation in the brain and the fact that participants were performing a Stroop task, these results also suggest that these differences reflect implicit rather than explicit attentional differences between lonely and nonlonely individuals. Source estimates were performed for purposes of hypothesis generation regarding underlying neural mechanisms, and the results implicated the neural circuits reminiscent of orienting and executive control aspects of attention as contributing to these differences. Together, the results are in accord with the evolutionary model of loneliness.

© 2015 Elsevier Ltd. All rights reserved.

Abbreviations: CENA, Chicago Electrical NeuroImaging Analytics; CI, Confidence interval; EEG, Electroencephalogram; ERP, Event-related potentials; GFP, Global field power; GSN, Geodesic Sensor Net; ICA, Independent component analysis; pAm, picoampere-meters; RMSE, Root mean square error; wMNE, weighted minimum-norm current estimate.

* Corresponding author. HPEN Laboratory, Center for Cognitive and Social Neuroscience, 940 E. 57th Street, Chicago, IL, 60637, USA.

E-mail address: scacioppo@bsd.uchicago.edu (S. Cacioppo).

1. Introduction

Fish on the edge of the group are more likely to be attacked by predators, not because they are the slowest or weakest, but because of the ease of isolating and preying upon those on the social perimeter (Ioannou, Guttal, & Couzin, 2012). As a result, fish have evolved to swim to the middle of the group when a predator attacks. Social isolation from a preferred partner has been shown to increase vigilance for threats in mammals, as well. For instance, prairie voles when isolated from their pair-bonded partner and subsequently placed in an open field, show less exploratory behavior and more predator evasion than prairie voles who have been housed with their partner (Grippo et al., 2014). Life on the social perimeter is dangerous for social animals and has detectable effects on attention and behavior, and perceived social isolation (or what has been termed loneliness in humans) activates neural, neuroendocrine, and behavioral responses that promote short-term survival (Cacioppo, Cacioppo, Capitanio, & Cole, 2015; Cacioppo, Capitanio, & Cacioppo, 2014).

Evidence from behavioral studies suggests that loneliness in humans affects early attentional processes to negative social stimuli (e.g., social threats). For instance, using a modified emotional Stroop task, lonely subjects, relative to nonlonely subjects, showed greater Stroop interference specifically for negative social relative to negative nonsocial words (Egidi, Shintel, Nusbaum, & Cacioppo, 2008). Stroop interference has been used to gauge the implicit processing of stimuli, so these results suggest that loneliness is associated with a heightened accessibility of negative social information. Similarly, in an investigation of the effects of subliminal priming on the detection of painful facial expressions, Yamada and Decety (2009) found that loneliness was associated with greater sensitivity to the presence of pain in disliked faces, as gauged by the sensitivity index, d' , from signal detection theory. In an eye tracking study, lonely and nonlonely young adults viewed various positive and negative social scenes and exhibited different fixation patterns. Individuals high in loneliness were more likely to first fixate on and to spend a greater proportion of their initial viewing time looking at socially threatening stimuli in a social scene, whereas individuals low in loneliness were more likely to first fixate on and spend a greater proportion of their initial view time looking at positive stimuli in a social scene (Bangee, Harris, Bridges, Rotenberg, & Qualter, 2014).

Functional magnetic resonance imaging (fMRI) research is also consistent with a heightened attention to social threats in the lonely brain. For instance, loneliness was directly related to the level of activation of the visual cortex in response to negative social images, in contrast to negative nonsocial images, whereas loneliness was inversely related to the level of activation of the temporal parietal region bilaterally, possibly reflecting less focus on others and more on one's own self-preservation in negative social contexts. On the other hand, a region associated with reward and appetitive behavior (i.e., ventral striatum) was more strongly activated in nonlonely than lonely individuals when exposed to pleasant social pictures in contrast to pleasant nonsocial pictures (Cacioppo,

Norris, Decety, Monteleone, & Nusbaum, 2009; cf. Cacioppo, Capitanio, et al., 2014).

The hypersensitivity to negative social information and the diminished pleasure derived from positive social stimuli might be expected to shape social expectations and motivations and contribute to a downward spiraling of negative affect and depressive symptomatology. Indeed, loneliness is related to stronger expectations of and motivations to avoid bad social outcomes and weaker expectations of and motivations to approach good social outcomes (Gable, 2006). Furthermore, loneliness, anxiety, and depressive symptoms are distinct states both by measures of statistical (Cacioppo et al., 2006; Capitanio, Hawley, Cole, & Cacioppo, 2014) and functional independence (Adam, Hawley, Kudielka, & Cacioppo, 2006; Cacioppo, Fowler, & Christakis, 2009; Kurina et al., 2011; Wilson et al., 2007). Furthermore, experimental research has shown that manipulations of loneliness lead to changes in anxiety and depressive symptomatology (Cacioppo et al., 2006), and longitudinal research on depression has shown that loneliness predicts increases in depressive symptomatology above and beyond what can be explained by basal levels of depressive symptomatology and demographic variables (Cacioppo, Hawley, & Thisted, 2010; Heikkinen & Kauppinen, 2004; VanderWeele, Hawley, Thisted, & Cacioppo, 2011).

Although fMRI studies provide valuable information about the neural correlates of social information processing in lonely and nonlonely brains, these studies are limited in the temporal information they provide and, when sample sizes are small, fMRI studies can be plagued by both Type I (false positives) and Type II (false negatives) errors (Button et al., 2013; Cacioppo, Frum, et al., 2013). Using high-density electrical neuroimaging, our main goal in the present investigation was to investigate the spatio-temporal brain dynamics evoked by the social Stroop task in lonely and nonlonely individuals. Specifically, we combined high-density electrical neuroimaging with a novel suite of event-related potential (ERP) analytic tools (Cacioppo, Weiss, Runesha, & Cacioppo, 2014) that allows not only the identification of standard ERP components but also the identification of the stable brain microstates specifically evoked by the social Stroop task in lonely and nonlonely individuals. Compared to the standard waveform analysis of ERP components that provides local information about amplitude and latency of the brain electric signal collected from one electrode in response to a stimulus, a brain microstate approach provides general information about the stable momentary configuration of the global scalp electric potential over a multichannel electrode array (Khanna, Pascual-Leone, Michel, & Farzan, 2015 for review). Along these lines, the brain microstate approach complements the traditional approach of ERP peaks and troughs at specific electrode positions with more comprehensive analyses of time-varying activity across the entire scalp (Cacioppo, Weiss, et al., 2014). More precisely, the brain microstate approach provides information about the brain activity associated with the sequence of discrete (and putatively non-periodic) information processing operations evoked by the presentation of a stimulus within the context or a particular experimental task, with exogenous ERP components sensitive to the

characteristics of the stimulus and endogenous ERP components sensitive to the stimulus in the context of the task. This sequence (or syntax) of information processing is composed of a series of stable brain microstates, each of which is characterized by the performance of specific cognitive computations and a relatively stable spatial distribution of brain activity. Each brain microstate may remain significantly stable for a certain amount of time (e.g., for tens to hundreds of milliseconds), and then changes into another brain microstate that remains stable again (e.g., Decety & Cacioppo, 2012; Cacioppo, Bianchi-Demicheli, et al., 2013; Michel, Seeck, & Landis, 1999; Ortigue, Sinigaglia, Rizzolatti, & Grafton, 2010). This approach suggests that the global pattern of brain electrical activity is modeled as being composed of a time sequence of decomposable brain microstates (Cacioppo, Weiss, et al., 2014; Khanna et al., 2015; Lehmann & Skrandies, 1980; Pascual-Marqui, Michel, & Lehmann, 1995).

Since the introduction of brain microstates in the 1980s (Lehmann & Skrandies, 1980), efforts have been made to improve the detection of brain microstates (Cacioppo, Weiss, et al., 2014). For decades, brain microstates have been identified using data clustering techniques (e.g., k-means cluster analysis) on the group-averaged ERPs of each experimental condition to identify the start, end, and nature of each brain microstate. The recent advances in computational neuroscience are offering new and more rigorous ways to identify automatically stable brain microstates (Cacioppo, Weiss, et al., 2014; Khanna et al., 2015 for review). In the present paper, we use a method that benefited from such advances in computational neuroscience i.e., the Chicago Electro-Neuroimaging Analytics (CENA; Cacioppo, Weiss, et al., 2014). Unlike previous methods of segmentation (e.g., based on k-cluster analyses) that require the a priori specification of the number of stable microstates in an ERP and the entire ERP is parsed into one of the specified number of microstates, the identification of brain microstates in CENA is data-driven, and the ERP is parsed into the baseline state, stable microstates, and non-stable transitions between these states (see Section 2.8 below for more details; Cacioppo, Weiss, et al., 2014).

Using CENA, the present study was conceptualized to investigate how fast loneliness (perceived social isolation) modulated a person's implicit attention to negative social information. Although a few EEG studies have been done previously on the automatic effects of social isolation (e.g., in humans' sleep EEG; Gemignani et al., 2014; in awakened human's EEG as measured with alpha frequency, Zubek, Bayer, & Shepard, 1967; in awakened Beagle pups' EEG, Fox, 1967; For reviews: Cacioppo & Patrick, 2008; Rasmussen, 1973, pp. 48; Cacioppo, Cacioppo, et al., 2015), little is known about the spatio-temporal dynamics of the automatic detection of social threat in the brain of individuals high versus low in loneliness. In sum, to test the experimental hypothesis that the implicit attention to negative social, in contrast to non-social, information differs between individuals high versus low in loneliness, we used CENA to perform a microstate analysis of high density EEG data to investigate the microstate timing and structure. Finally, source localization was performed for each microstate for purposes of hypothesis generation.

2. Material and methods

2.1. Experimental design and subjects

The experimental design was a $2 \times 2 \times 2$ mixed-model factorial design with Word Type (social; nonsocial) and Word Valence (positive; negative) as within-subjects factors, and Loneliness (high; low) as a between-subjects factor. The order of conditions was varied across subjects. Subjects also performed a standard Stroop task after they completed the social and emotional Stroop tasks reported here. EEG analyses of these data fall outside the scope of the current paper, though behavioral analyses of the standard Stroop task confirmed the classic Stroop interference effect ($p < .001$; partial eta squared = .23), with the color of color words identified more slowly ($M = 736.03$; $SD = 141.14$) than the color of non-words ($M = 651.42$; $SD = 129.89$).

A total of 105 individuals volunteered to participate in the study, for which they received \$15 per hour. Subjects were pre-screened by email using the R-UCLA loneliness scale (Russell, 1996), which consists of 20 items measuring general loneliness (without ever using the word "lonely" or "loneliness") and degree of satisfaction with one's social relationships. Subjects responded on a 4-point Likert scale that indicates the frequency with which they feel this way from 1 (never) to 4 (often). Total scores can range from 20 to 80, and any subject whose total score was 41 or higher was recruited for the high lonely group, and any subject whose total score was less than 41 was recruited for the low lonely group. Subjects were not aware that loneliness was measured in the pretest or that the study concerned loneliness per se.

Because of errors in recordings or poor signal-to-noise ratio in EEG data, recordings for 30 subjects were not included in the analyses. Errors with the behavioral paradigm caused the loss of data from two additional subjects, and data from three additional subjects were not considered because their accuracy level for color identification was at or below chance levels. This led to a total of 70 subjects (mean age = 23.59, $SD = 5.62$), 38 of whom (17 women and 21 men) were high in loneliness ($M = 48.00$, $SD = 6.68$) and 32 of whom (13 women, 19 men) were low in loneliness ($M = 31.91$, $SD = 5.08$).

All subjects were native English speakers, undergraduate, graduate or medical students at the University of Chicago, who had normal or corrected to-normal visual acuity. Sixty-four of the 70 subjects were right-handed and six of them were left-handed (Edinburgh Handedness Inventory, Oldfield, 1971). None had any prior or current neurological or psychiatric impairment, as ascertained by a detailed anamnesis. The anamnesis included an assessment of the subject's feelings of anxiety and depression (Zigmond & Snaith, 1983), and on average subjects scored within normal ranges on both measures ($M_{\text{anxiety}} = 5.20$, $SD = 2.63$; $M_{\text{depression}} = 4.64$, $SD = 2.35$).

2.2. Procedure

First, experimenters read the local Institutional Review Board-approved study information script to the volunteers upon their arrival at the High Performance Electrical Neuroimaging (HPEN) laboratory. This script informed the subjects about the

procedure of the experiment and asked them whether they were willing to give oral consent for their participation. Once subjects gave their oral consent, they completed the anamnesis and handedness questionnaire, and the experimenter applied a 128-sensor EEG net. After the sensor net was placed on subjects and an impedance level of $100 \text{ k}\Omega$ or lower had been achieved for all sensors, subjects performed a short behavioral task designed to allow them to memorize the placement of colors on the response keypad, and the Stroop task was explained to the subject. The experimenters never referred to loneliness when describing the study. Upon completion of the Stroop task, subjects were debriefed, paid, and allowed to ask questions.

2.3. Subjects' instruction

Subjects were instructed to indicate, as quickly and as accurately as possible, the color of the ink of each centrally-presented string of letters by pressing one of four keys (labeled with corresponding color panes: red, green, blue, or yellow) with the four fingers (index to pinkie) from their right hand. In addition, subjects were instructed to gaze at the center of the screen and to refrain from blinking or moving their eyes except during the interval between trials (Cf. [Supplementary information](#) for details). After each subject's response, the string of letters disappeared from the center of the screen and the experiment continued to the next trial.

2.4. Experimental paradigm

Words were blocked by category. The subjects viewed a total of seven experimental blocks: One practice block and six experimental blocks. Subjects saw one of two ordering of the experimental blocks. The first order was Positive Social, Emotional Negative, Emotional Positive, Negative Social, Color (classic Stroop), and Control (XXXXX), and the second order was Emotional Positive, Negative Social, Positive Social, Emotional Negative, Color, and Control.

The practice block consisted of 6 words (HOLIDAY, GLASS, CARPET, CAKE, BAND, CONCENTRATE) presented once and 1 word (CHAIR) presented twice during the block in each of four different ink colors (red, blue, green, & yellow). Order of the stimuli was randomized, yielding a total of 32 practice trials. Each experimental block including emotional or social words contained 10 words (See [Table 1](#)) that were repeated four times, once in each of four ink colors, with the order of the stimuli randomized across the 40 trials. Each letter string was presented in the same upper case, sans-serif font with a 48-point size on a black background. In each block, the letter strings were presented centrally one by one, while the subjects' brain activity was recorded. This entire experiment was carried out using E-Prime 2.0.8.90 software (Psychology Software Tools, Pittsburgh, PA).

2.5. Selection of stimuli

A list of 125 words selected from the ANEW Instruction Manual and Affective Ratings ([Bradley & Lang, 1999](#)) were presented in an online survey on Amazon Mechanical Turk where 100 subjects rated each word's emotional, social,

Table 1 – List of social and emotional stimuli (Alphabetical order).

Social positive	Social negative	Emotional positive	Emotional negative
ACCEPTED	ALONE	BRAVE	ANGRY
ADMIRE	DETACHED	ENJOY	ANXIOUS
BELONG	DISLIKED	HAPPY	DEPRESSED
FRIENDLY	EXCLUDED	JOY	FEAR
INCLUDED	FOE	JOYFUL	FRUSTRATED
INVITED	HOSTILE	LUCKY	MISERY
LIKED	ISOLATED	PLEASED	PANIC
PAL	REJECTED	PLEASURE	SAD
PARTY	SOLITARY	SUCCESS	STRESS
SQUAD	UNWANTED	SURPRISED	VOMIT

arousal, and valence content on a scale from 0 to 7 (0 = extremely low; 7 = extremely high). No reaction times (RTs) were collected in this Mechanical Turk survey. From this online survey, 60 words (30 emotional [15 positive and 15 negative] and 30 social [15 positive and 15 negative] words) were selected. Two experimenters (SC and ABB) made this selection. Words defined as social reflected social interactions or feelings of isolation/connectedness related to social interactions (e.g., rejected, accepted). In contrast, nonsocial words could apply to various emotions (e.g., joy, sad) even in the absence of social interactions. To ensure the two experimenters chose words that were unequivocally considered as being emotional or social by experts in social psychology, the list of 60 words was then given to a social psychologist (J. Cloutier), who rated each word as being either social or emotional in a blind manner (he was not aware of the exact pre-categorization from the two experimenters). From this categorization, two experimenters (SC and JTC) selected 10 words that had been selected to be and had been rated as either emotional or social ([Table 1](#)). Statistical analyses were conducted on these 10 words to ensure that a) all word category (emotional positive, emotional negative, Positive Social, and Negative Social) had comparable average word lengths, b) positive social words did not differ from positive emotional words in valence ratings, c) negative social words did not differ from negative emotional words in valence ratings d) social words were rated as more social than emotional words, and e) emotional words were rated as more emotional than social words. No significant difference was found between the four types of words in terms of word length [$F(3, 36) = .811; p = .496$; [Table 2](#)], between positive social words and positive emotional words in valence ratings [$t(18) = 1.271, p = .22$] or word frequencies [[Kucera & Francis, 1967](#); $t(18) = -.660, p = .52$], and between negative social words and negative emotional words in valence ratings [$t(18) = -1.707, p = .11$] or word frequencies [$t(18) = -.279, p = .78$]. Social words were also rated as more social than emotional words [$t(38) = -3.60, p = .001$], and emotional words were rated as more emotional than social words [$t(38) = 3.82, p = .000$]. No significant difference was found between social and emotional words in terms of arousal [$t(38) = 1.15, p = .257$]. Finally, the analysis of RTs revealed no significant differences between social and nonsocial conditions in the two groups of participants. These results indicate that the manipulations were effective. Thus, the speed of processing was similar in the two conditions.

Table 2 – Mean social, emotional, arousal, and valence contents on a scale from 0 to 7 (0 = extremely low, 7 = extremely high) and average word length for each word category.

Category	Social	Emotional	Valence	Arousal	Word length
Social positive	5.79 (.39)	4.37 (.85)	5.46 (.47)	3.92 (.48)	6.2 (1.69)
Social negative	3.34 (.33)	4.76 (.62)	2.35 (.37)	2.56 (.23)	7.1 (1.73)
Emotional positive	4.04 (.19)	5.41 (.63)	5.69 (.34)	4.48 (.30)	6 (1.76)
Emotional negative	2.65 (.35)	5.52 (.87)	2.13 (.18)	2.65 (.29)	6 (2.16)

2.6. Data acquisition and analysis

Continuous electroencephalogram (EEG) was recorded from 128 AgCl carbon-fiber coated electrodes using an Electric Geodesic Sensor Net® (GSN300; Electrical Geodesic Inc., Oregon; <http://www.eeg.com/>), where EEG electrodes are arrayed in a dense and regular distribution across the head surface with an inter-sensor distance of approximately 3 cm. The EEG was digitized at 250 Hz (corresponding to a sample bin of 2 msec), band-width at .01–200 Hz, with the vertex electrode (Cz) serving as an on-line recording reference; and impedances were kept below 100 kΩ.

RTs and accuracy were recorded from a Windows XP (Service Pack 3) computer running E-Prime 2.0.8.90 software (Psychology Software Tools, Pittsburgh, PA). All subjects were seated so that their eyes were level with the location of the stimuli. Due to the skew inherent in RT measures, all word category RT time means were transformed using a square root function. An interference score for negative stimuli was then computed by subtracting the mean RT for negative nonsocial words from that of negative social words, and an interference score for positive stimuli was computed by subtracting the mean RT for positive nonsocial words from that of positive social words.

2.7. Electrophysiological image preprocessing

Electrophysiological data were imported and analyzed using ERPLAB (version 4.0.2.3; Steve Luck and Javier Lopez-Calderon, University of California at Davis), and EEGLAB (version 13.1.1; Arnauld Delorme and Scott Makeig, UCSD), with additional analysis done using Cartool (version 4.53; Denis Brunet; <http://brainmapping.unige.ch/Cartool.htm>). Electrical data were band-pass filtered between .1 and 30 Hz, and notch filtered at 60 Hz to remove any residual interference. Independent Component Analysis (ICA) weights were calculated to compute 128 components for each experimental block (using the RUNICA algorithm and EEGLAB functionality); these components were then visually inspected, and the datasets were purged of independent components related to eye blink artifacts. Epochs of analysis were defined so as to end 1000 msec after onset of visual stimuli, and contained a 300 msec pre-stimulus baseline. Epochs were visually inspected for oculomotor (saccades, and blinks), muscles, and

other artifacts in addition to an automated threshold rejection criterion of 100 µV. After off-line artifact rejections, ERPs were computed covering the 1300 msec epoch length. Channels with corrupted signals and channels showing substantial noise throughout the recording were interpolated to a standard 111-channel electrode array using a three-dimensional spline procedure (Perrin, Pernier, Bertnard, Giard, & Echallier, 1987).

2.8. Second-level electrophysiological analysis

Group-averaged data were subsequently processed using The Chicago Electro-Neuroimaging Analytics (CENA) suite (Cacioppo, Weiss, et al., 2014; <https://hopenlaboratory.uchicago.edu/page/cena>) to identify brain microstates. The notion of discrete brain microstates was introduced in the 1980's by Lehmann to refer to periods of stable (from tens to hundred milliseconds) event-related brain response (Lehmann, 1987). To detect these brain microstates, four quantitative methods were applied to the ERP time series across the 128-sensor space: (1) a root mean square error (RMSE) metric and a 99% confidence interval (CI) for identifying potential stable brain microstates; (2) a global field power (GFP) and a 99% CI for identifying changes in the overall level of activation of the brain; (3) a similarity metric based on cosine distance and a 95% CI to determine whether template maps for successive brain microstates differ in configuration of brain activity, global field power, or a combination of the two; and (4) a bootstrapping procedure for assessing the extent to which the solutions identified in the micro-segmentation are robust (reliable, generalizable) and for empirically deriving additional experimental hypotheses (Cacioppo, Weiss, et al., 2014). The present investigation focused on event-related microstates, as determined by the RMSE metric and the similarity metric based on cosine distance.

CENA has several advantages over prior methods for segmenting the ERP. For instance, unlike previous methods of segmentation (e.g., based on k-cluster analyses) that require the a priori specification of the number of stable microstates in an ERP and the entire ERP is parsed into one of the specified number of microstates, the identification of brain microstates in CENA is data-driven, and the ERP is parsed into the baseline state, stable microstates, and non-stable transitions between these states. The applied version of CENA (version 2014-09-23; Cacioppo, Weiss, et al., 2014) was implemented as a plugin in Brainstorm (version 3.2; Tadel, Baillet, Mosher, Pantazis, & Leahy, 2011).

2.9. Distributed cortical source estimation

As a final step, we estimated the brain generators of every stable microstate using a cortical source estimation package implemented in Brainstorm (Tadel et al., 2011). Specifically, we used the forward model that was calculated with a symmetric Boundary Element Model (Gramfort, Papadopoulou, Olivi, & Clerc, 2010; Kybic et al., 2005) generated with OpenMEEG on the cortical surface of a template MNI brain (colin27 atlas) with a 1 mm resolution (Collins et al., 1998; Tzourio-Mazoyer et al., 2002). Cortical source estimations (in picoampere-

meters; pA m) were i) estimated with a constrained inverse model of EEG sources using the standard weighted minimum-norm current estimate (wMNE; Baillet, Mosher, & Leahy, 2001) and ii) mapped to a distributed source model consisting of 15,002 elementary current dipoles, as implemented in Brainstorm. The source activity at each cortical location was standardized using the z-score transformation with respect to the average and standard deviation of the source activity during baseline: a 300-msec time window in the pre-response period.

2.10. Statistical analysis plan

As outlined in Cacioppo, Weiss, et al. (2014), potential event-related microstates are initially identified in CENA based on an RMSE metric using a lag of 12 msec, a baseline period from which to calculate the noise in the ERP configuration ranging from -284 msec pre-stimulus to 48 msec post-stimulus, and a 99% CI to detect significant rises or falls in the RMSE function. The series of potential microstates identified across an ERP waveform were then subjected to a cosine metric analysis using a 95% CI to determine whether the $n+1$ st microstate differed significantly in configuration from the n th microstate (see Cacioppo, Weiss, et al., 2014).

In the present research, a priori orthogonal contrasts were conducted to determine differences between individuals high or low in loneliness in the event-related microstates elicited by negative social and nonsocial words during the Stroop task, and a parallel set of orthogonal contrasts were conducted to determine differences between individuals high or low in loneliness the event-related microstates elicited by positive social and nonsocial words during the same Stroop task. The 2 (Loneliness: high, low) \times 2 (Word Type: Social, Nonsocial) contrasts for the negative (positive) stimuli were performed using CENA as follows.

In Fig. 1, A represents the between-subjects factor (Loneliness), a_1 represents low loneliness, a_2 represents high loneliness, B represents the within-subjects factor (Word Type), b_1 represents Negative Social words, and b_2 represents Negative Nonsocial words to which subjects were exposed during the Stroop task. The topographical maps (topo-maps) for the Grand Mean were first inspected for artifacts or bad channels in the recordings. [The Grand Mean is used because it generally represents the best estimate of integrity of the ERP recordings across time and it avoids any confirmatory bias in editing based on any expected differences between conditions.] In addition, it was verified that the same number of trials from a given subject contributed to each cell of the within-subjects design.

The main effect test for A (Loneliness) was determined through the following steps using the CENA plug-in available for Brainstorm: (1) average the a_1b_1 and a_1b_2 topo-maps to create the topo-maps for Mn_a_1 ; (2) average the a_2b_1 and a_2b_2 topo-maps to create the topo-maps for Mn_a_2 ; (3) difference the Mn_a_1 and Mn_a_2 topo-maps to create the topo-maps for the Main Effect for A [i.e., calculate (1)-(2)]; (4) average the Mn_a_1 and Mn_a_2 topo-maps to create the topo-maps for the Grand Mean [i.e., average (1) and (2)]; (5) perform the CENA on (1) to create the microsegmentation (and template maps) for Mn_a_1 ; (6) perform the CENA on (2) to create the microsegmentation (and template maps) for Mn_a_2 ; (7) perform the

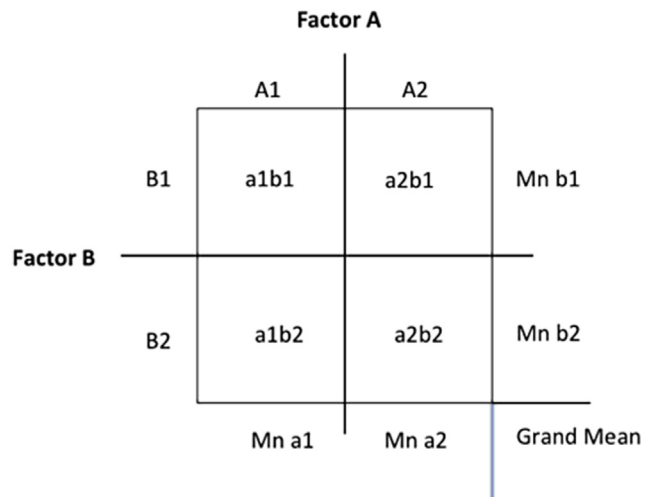


Fig. 1 – Schematic representation of Factors A and B. A represents the between-subjects factor (Loneliness), a_1 represents low loneliness, a_2 represents high loneliness, B represents the within-subjects factor (Word Type), b_1 represents Negative Social words, and b_2 represents Negative Nonsocial words to which subjects were exposed during the Stroop task.

CENA on (3) to create the microsegmentation (i.e., epochs of significant difference) between Mn_a_1 and Mn_a_2 – that is, for the periods of time in which the brain microstates differed as a function of Factor A; (8) perform the CENA on (4) to create the microsegmentation for the periods of time in which the brain microstates did not differ as a function of Factor A; and (9) in the penultimate step, use the results of (7) when comparing (5) with (6) to determine the epochs during which the evoked brain microstates in Mn_a_1 and Mn_a_2 differ statistically.

(9a) For the epochs in which (7) shows no significant differences between (5) and (6), refer to (8) to characterize the evoked brain microstates across Factor A. For such an epoch, source localization (see Section 2.10) is performed on the observed microstate(s) during this epoch in the Grand Mean [i.e., (8)].

(9b) For the epochs in which (7) shows significant differences between (5) and (6), refer to (5) and (6) to characterize the distinct evoked brain microstates as a function of Factor A. For such an epoch, source localization is performed on the observed microstate(s) during this epoch separately in (4) and in (5).

The main effect test for B (Word Type) was determined using an analogous set of steps as used for the main effect test for A. Here, Factor A (Loneliness) was the between-subjects factor and Factor B (Word Type) was the within-subjects factor, so the simple main effect tests would be calculated within each level of A.

The $A \times B$ interaction test was performed through the following steps: (1') difference the a_1b_1 and a_1b_2 topo-maps to create the topo-maps for the simple main effect for a_1 ; (2') difference the a_2b_1 and a_2b_2 topo-maps to create the topo-maps for the simple main effect for a_2 ; (3') calculate (1') –

(2') to create the topo-maps for the $A \times B$ interaction (i.e., difference of the differences); (4') average the Mn_a1 and Mn_a2 topo-maps to create the topo-maps for the Grand Mean [this average should be available from (4) above]; (5') perform the CENA on (1') to create the microsegmentation (and template maps) for the simple main effect for a1; (6') perform the CENA on (2') to create the microsegmentation (and template maps) for the simple main effect for a2; (7') perform the CENA on (3') to create the microsegmentation (i.e., epochs of significant difference) between the simple main effects for a1 and for a2 – that is, for the periods of time during Factors A and B interacted to produce the observed brain microstates; (8') access the CENA for the Grand Mean, the Main Effect for Factor A, and the Main Effect for Factor B to aid in the following steps; and (9') in the penultimate step in this analysis, use the results of (7') when comparing (5') with (6') to determine the epochs during which the evoked brain microstates in simple main effect a1 and simple main effect a2 differ statistically – that is, the epochs for which there was a significant interaction between Factors A and B.

(9a') For the epochs in which (7') shows no significant differences between (5') and (6'), refer to (8') to characterize the evoked brain microstates. Given there is no $A \times B$ interaction during this epoch, inspection of the results in (8') best specify the microstate structure during this epoch. If main effects were also absent for this epoch, then source localization is performed on the observed microstate(s) during this epoch in the Grand Mean. If the main effect for Factor A and/or Factor B is significant for this epoch, then refer to the results above to characterize the evoked brain microstate(s) observed during this epoch.

(9b') For the epochs in which (7') shows significant differences between (5') and (6'), refer to (5') and (6') to characterize the distinct evoked brain microstates as a function of Factors A and B. For such an epoch, source localization should be performed on the observed microstate(s) during this epoch separately in (4') and in (5'). Pairwise comparisons between and source localization within each cell (e.g., a1b1, a1b2, a2b1, & a2b2) may also be performed as a means of breaking down the interaction to all possible pairwise comparisons.

The main effect tests are constructed prior to the interaction test because the latter requires waveforms constructed when testing main effects. However, the interpretation of the results begins with the interaction test to determine what periods of the ERP differ significantly, and what is the microstate(s) that are responsible for any such differences. The use of orthogonal contrasts and 95% and 99% CIs maintain an alpha error of less than .05 in the results reported below.

3. Results

3.1. Negative social and nonsocial words

The Word Type \times Loneliness interaction test revealed a significant difference for the period ranging from 280 to 960 msec and again from 976 msec to the end of the recording epoch (i.e., 1000 msec). The ERP waveform in 128 dimensional sensor space was next investigated within subjects high in loneliness and within subjects low in loneliness. As noted above, these

simple effects tests were performed within-subjects to ensure the ERP waveform as a function of Word Type was examined: (a) within the same set of subjects/brains, and (b) across average waveforms calculated from the same number of trials.

The first simple effects test focused the contrast between Negative Social and Negative Nonsocial Words in subjects *high* in loneliness. The contrast revealed significant differences in the two ERP waveforms as a function of Word Type for the period ranging from 280 to 1000 msec. Consequently, the microstate structure prior to 280 msec was defined based on analyses of the ERP collapsed across Word Type within subjects high in loneliness, and the microstate structure after 280 msec was defined based on analyses of the ERP within Word Type for subjects high in loneliness. The statistically significant results ($p < .05$), which are depicted in the top panel of Fig. 2, showed that in the first 280 msec the same three discrete microstates are evoked in the Negative Social Word and Negative Nonsocial Word conditions. Three additional discrete microstates follow in the Negative Social Word condition, whereas two additional discrete microstates follow in the Negative Nonsocial Word condition. For instance, the first of these later evoked microstates was evoked over similar periods (280–800 msec in the Negative Social Word condition and 280–768 msec in the Negative Nonsocial Word condition), but these microstates differed significantly across the 128-sensor space ($p < .05$, as determined by the RMSE and cosine metrics; Cacioppo, Weiss, et al., 2014).

Although the new quantitative procedure for identifying stable event-related brain microstates introduced here may serve as a better basis for source localization estimates in part because it differentiates stable brain microstates from transitions between states (Cacioppo, Weiss, et al., 2014), it is worth noting that the inferences drawn from the source analysis in this paper are for purposes of hypothesis generation – not hypothesis testing. The results are illustrated in the bottom panel of Fig. 2 and are summarized in Table 3.

During the first three microstates elicited by negative words in the Stroop task within the first 280 msec – three microstates that did not differ for negative social and non-social words—the brain source localization revealed a bilateral activation in visual brain areas. More precisely, inspection of Table 3, for instance, shows that the first microstate, which ranged from 108 to 120 msec, reflected activation of the extrastriate cortex (BA18, BA19) and fusiform gyrus (BA37). The second microstate, which lasted between 152 and 180 msec, revealed activation in the left primary somatosensory cortex, the right inferior temporal gyrus, and bilateral fusiform gyrus. The third microstate, which extended from 220 to 280 msec, included the extrastriate cortex, precuneus, and anterior prefrontal cortex extending to the dorsal anterior cingulate cortex.

Then, both the negative social and negative nonsocial stimuli elicited a fourth microstate beginning approximately 280 msec post-stimulus, and these microstates manifested over similar periods of time (280–800 msec for negative social words & 280–768 msec for negative nonsocial words); however, these microstates differed significantly in the pattern of activity recorded over the 128-sensor space. Comparison of

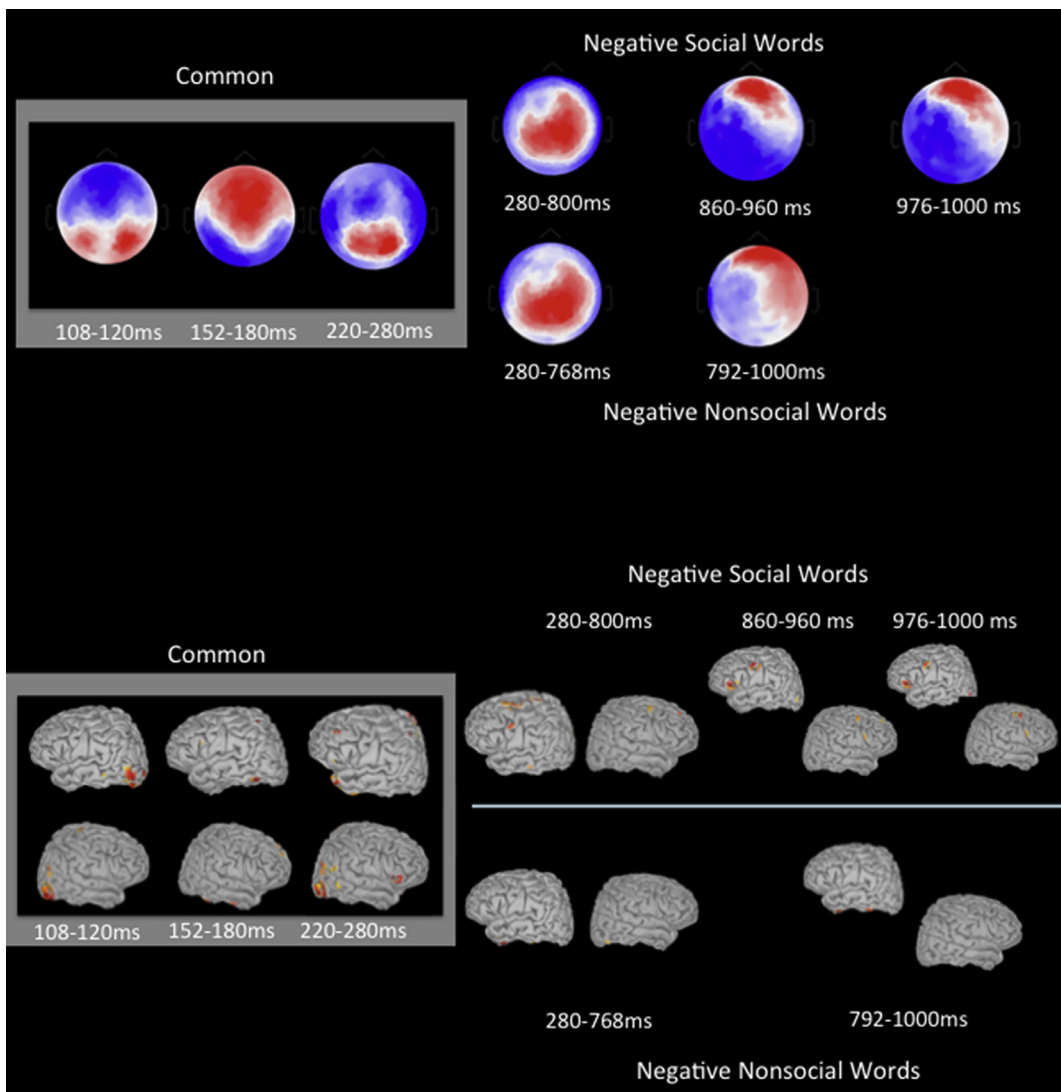


Fig. 2 – Brain microstates evoked in individuals high in loneliness in response to negative social and nonsocial words in the Stroop task. Top panel: Template maps for each discrete microstate. Bottom panel: Cortical source estimations were calculated for each discrete microstate.

brain source localization estimates for these microstates indicated that the negative social, in contrast to nonsocial, words in the Stroop task elicited activation in more brain regions involved in the orienting and executive control aspects of visual attention (e.g., extrastriate cortex, fusiform cortex, frontal eye field, dorsolateral prefrontal cortex; & anterior prefrontal cortex extending to the dorsal anterior cingulate; see Table 3).

The second simple effects test focused the contrast between Negative Social and Negative Nonsocial Words in subjects low in loneliness. As expected, the results indicated that the first five microstates (from 92 msec to 488 msec post-stimulus onset) elicited by the Stroop task were the same for negative social and negative nonsocial words, and source estimates of these microstates suggested the involvement in neural regions commonly found in fMRI studies of the Stroop task, including the anterior prefrontal cortex extending to

the dorsal anterior cingulate, the dorsolateral prefrontal cortex, and the secondary visual cortex (BA18) and associative visual cortex (BA19) within the extrastriate cortex (see Fig. 3; Table 4).

Then, for the period ranging from 490 to 1000 msec, three additional discrete event-related microstates followed in the Negative Social Word condition, and three discrete event-related microstates followed in the Negative Nonsocial Word condition. For instance, the first of these later evoked microstates in the Negative Social and Nonsocial Word conditions was evoked at a similar point in time (490 msec), but this state ended 50 msec later in the Negative Social Word condition whereas this microstate lasted much longer (394 msec) in the Negative Nonsocial Word condition. Specifically, the discrete microstates elicited by negative nonsocial words occurred between 490 msec and 884 msec, followed by two shorter microstates (900–968 msec, & 984–1000 msec), whereas the

Table 3 – Local maxima of current source density obtained from wMNE brain source estimations for High lonely in response to Social Negative Stimuli (in dark blue) versus Non-Social Negative Stimuli (in aqua blue).

Microstate time periods for Social Negative	Microstate time periods for Non-Social Negative	Brodmann Areas	Brain region labels	MNI		
				Brain coordinates		
				x	y	z
108-120 ms		BA18	Secondary visual cortex	-43	-90	-4
				40	-90	-4
		BA19	Associative visual cortex	45	-82	27
		BA37	Fusiform gyrus	-62	-57	-14
		BA6	Supplementary motor area (SMA)	-61	7	28
				-5	22	67
		BA10	Anterior prefrontal cortex	-5	66	-14
		BA 38	Middle temporal pole	-59	-1	-31
152-180 ms		BA 44	Inferior frontal gyrus	-62	16	22
		BA 46	Dorsolateral prefrontal cortex	50	41	2
		BA1	Primary somatosensory cortex	-51	-35	59
		BA20	Inferior temporal gyrus	42	-14	-38
		BA 37	Fusiform gyrus	-53	-70	-17
				61	-56	-25
		BA6	SMA	-37	10	58
		BA8	Frontal eye field	42	11	56
				-37	25	49
		BA9	Dorsolateral prefrontal cortex	12	61	30
		BA10	Anterior prefrontal cortex	-41	43	32
		BA18	Associative visual cortex	21	-104	3
				-16	-104	9
				-13	-90	28
		BA19	Associative visual cortex	-28	-90	28
		BA21	Middle temporal gyrus	63	-1	-28
				-61	-26	-17
		BA38	Middle temporal pole	-38	20	-40
		BA39	Angular gyrus	-41	-58	56

(continued on next page)

Table 3 – (continued)

Microstate time periods for Social Negative	Microstate time periods for Non-Social Negative	Brodmann Areas	Brain region labels	MNI		
				x	y	z
220-280 ms		BA18	Secondary visual cortex	37	-90	-5
				-41	-90	-2
		BA45	Inferior frontal gyrus (Pars triangularis)	60	27	0
		BA 7	Superior parietal lobule	-35	-57	64
				9	-57	74
		BA10	Anterior prefrontal cortex	-5	66	-14
		BA20	Inferior temporal gyrus	-53	-15	-40
		BA1	Primary somatosensory cortex	-39	-44	63
		BA8	Frontal eye field	15	34	57
		BA11	Orbito-frontal area	13	65	-15
280-800 ms		BA47	Inferior frontal gyrus (Pars orbitalis)	58	32	-4
				-52	27	-4
		BA10	Anterior prefrontal cortex	30	57	15
		BA18	Secondary visual cortex	31	-97	-14
		BA19	Associative visual cortex	27	-93	27
		BA20	Inferior temporal gyrus	-48	4	-39
				43	-19	-34
		BA21	Middle temporal gyrus	-71	-41	-7
		BA37	Fusiform area	24	-35	-18
				-67	-48	-18
		BA1	Primary somatosensory cortex	-60	-13	38
		BA6	SMA	-19	-19	75
				43	4	53
		BA8	Frontal eye field	41	9	57
		BA9	Dorsolateral Prefrontal Cortex	-9	51	39
				25	52	36
		BA38	Middle temporal pole	43	10	-44
		BA11	Orbito-frontal area	5	42	-12
280-768 ms		BA20	Inferior temporal gyrus	-54	-3	-38
		BA37	Fusiform gyrus	-62	-57	-24

Table 3 – (continued)

				56	-66	-18
		BA19	Associative visual cortex	48	-82	-15
	792-1000 ms	BA 37	Fusiform area	-64	-59	-22
		BA20	Ventral temporal pole	-54	-4	-37
		BA21	Middle temporal gyrus	-65	-29	-22
	860-960 ms	BA47	Inferior frontal gyrus (Pars orbitalis)	-55	33	-6
				45	45	-6
		BA6	SMA	45	4	54
				-57	3	42
		BA18	Secondary visual cortex	-41	-90	1
		BA45	Inferior frontal gyrus (Pars triangularis)	-56	36	5
				-55	36	-2
		BA8	Frontal eye field	-53	13	40
		BA10	Anterior prefrontal cortex	42	53	-15
		BA18	Secondary visual cortex	-40	-96	-3
				31	-96	-15
		BA20	Inferior temporal gyrus	-52	-4	-44
				66	-30	-26
		BA38	Middle temporal pole	-56	5	-35
		BA44	Inferior frontal gyrus (Pars opercularis)	-60	17	28
	976-1000 ms	BA47	Inferior frontal gyrus (pars orbitalis)	-56	34	-2
		BA6	SMA	-58	3	41
				43	3	57
		BA8	Frontal eye field	43	11	55
		BA18	Secondary visual cortex	-40	-90	1
		BA44	Inferior frontal gyrus (pars opercularis)	62	16	19
		BA10	Anterior prefrontal cortex	44	50	-4
		BA45	Inferior frontal gyrus (pars triangularis)	59	32	0

Local maxima are in MNI coordinates. The maxima with an amplitude greater than 70% (i.e., > 210 pAm, inclusive) are indicated in bold, while the local maxima with an amplitude greater than 51% (> 153 pAm, with a minimum size of 10) are provided in light grey in the table. Common microstate time periods are highlighted in dark grey. Microstate time periods specific to social stimuli are highlighted in dark blue, while microstate time periods specific to non-social stimuli are highlighted in aqua blue.

microstates elicited by negative social words ranged from 490 to 540 msec, 552–688 msec, and 780–1000 msec (see Fig. 3).

Finally, distributed cortical source estimation was performed to investigate the brain generators of these evoked microstates. The results are illustrated in the bottom panel of Fig. 3 and are summarized in Table 4. In brief, source localization estimates indicated that the microstates elicited by the nonsocial words were focused largely within the dorsolateral prefrontal cortex (a brain area known to be involved in Stroop task), whereas the microstates elicited by the social words in

the Stroop task reflected activation in a much more distributed set of brain regions, including those involved in orienting, theory of mind, and executive control aspects of attention and in social cognition (Table 4).

3.2. Positive social and nonsocial words

The Word Type × Loneliness interaction test revealed significant differences during five periods of the ERP waveform: (a) 136–608 msec, (b) 632–680 msec, (c) 696–756 msec, (d)

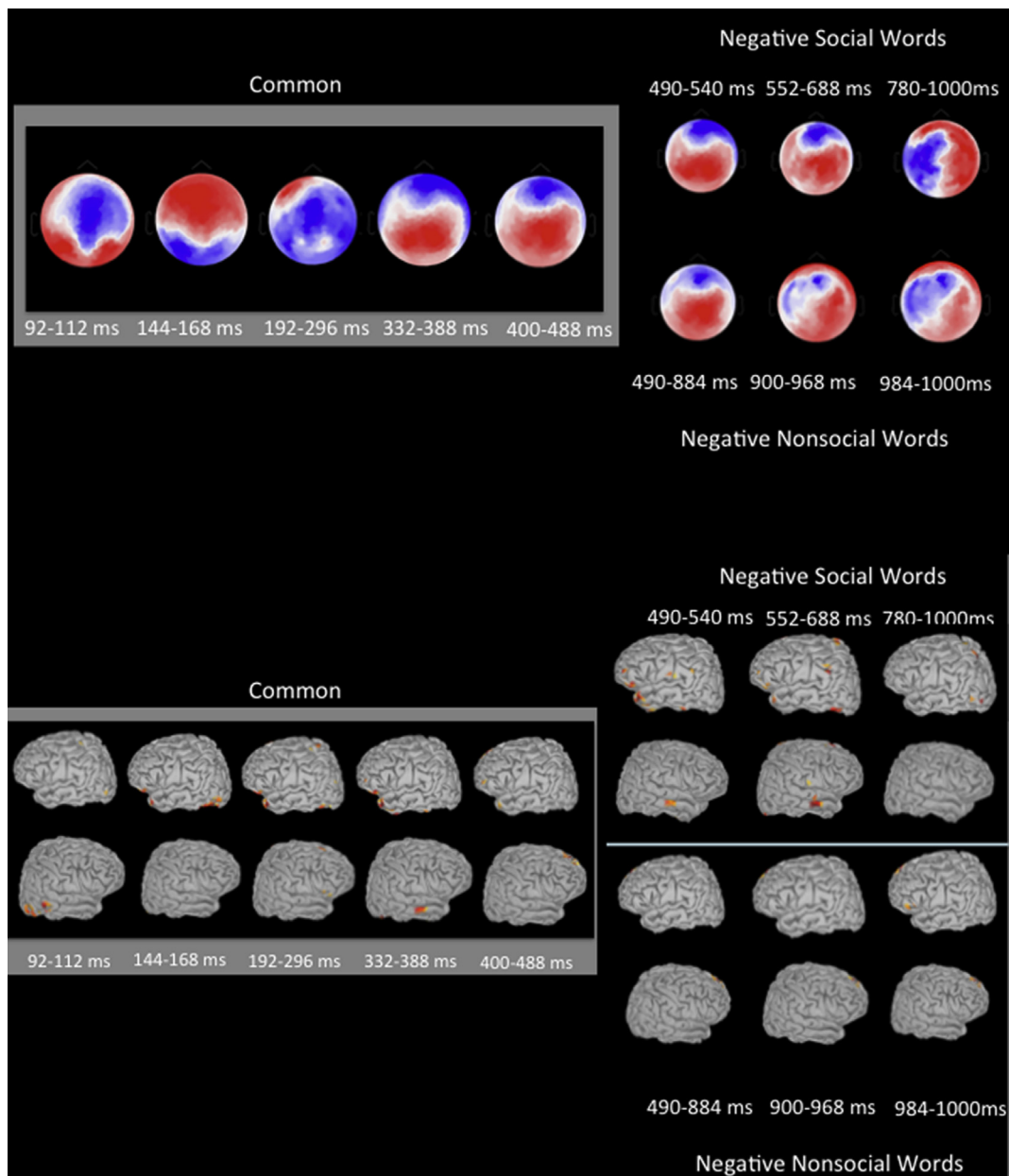


Fig. 3 – Brain microstates evoked in individuals low in loneliness in response to negative social and nonsocial words in the Stroop task. Top panel: Template maps for each discrete microstate. Bottom panel: Cortical source estimations were calculated for each discrete microstate.

768–784 msec, and (e) 800–1000 msec. The ERP waveform in 128 dimensional sensor space was next investigated within subjects *high* in loneliness and within subjects *low* in loneliness.

The first simple effects test focused on the contrast between Positive Social and Positive Nonsocial Words in subjects *high* in loneliness. The contrast revealed significant differences in the brain microstates elicited as a function of Word Type. The statistically significant results ($p < .05$), which are depicted in the top panel of Fig. 4, shows that four microstates were evoked by Positive Social Words, whereas three microstates were evoked by Positive Nonsocial Words

when subjects *high* in loneliness performed the Stroop task (see Fig. 4). More precisely, the positive nonsocial words elicited an initial microstate from 140 to 180 msec, a second much longer microstate that ranged from 216 to 792 msec, and a third microstate from 840 to 1000 msec, whereas the positive social words elicited an initial microstate from 152 to 184 msec, a second from 216 to 304 msec, a third from 328 to 680 msec, and a fourth microstate ranging from 696 to 1000 msec.

Finally, distributed cortical source estimation was performed to investigate the brain generators of these evoked microstates. The results are illustrated in the bottom panel of

Table 4 – Local maxima of current source density obtained from wMNE brain source estimations for Low lonely in response to Social Negative Stimuli (in dark blue) versus Non-Social Negative Stimuli (in aqua blue).

Microstate time periods for Social Negative	Microstate time periods for Non-Social Negative	Brodmann Areas	Brain region labels	MNI Brain coordinates			
				x	y	z	
92-112 ms			BA18	Secondary visual cortex	40	-93	1
					-42	-90	1
			BA19	Associative visual cortex	52	-78	1
			BA37	Fusiform gyrus	65	-58	1
			BA1	Primary somatosensory cortex	-31	-35	73
			BA7	Superior parietal lobe	-29	-43	68
			BA19	Associative visual cortex	-28	-87	29
			BA21	Middle temporal gyrus	67	-40	3
			BA39	Angular gyrus	-31	-80	42
144-168 ms			BA18	Secondary visual cortex	-35	-91	-15
			BA37	Fusiform gyrus	-56	-66	-19
			BA38	Temporopolar area	-50	18	-31
			BA47	Inferior frontal gyrus (pars orbitalis)	-49	35	-15
			BA20	Inferior temporal gyrus	65	-26	-24
			BA8	Frontal eye field	10	35	58
192-296 ms			BA19	Associative visual cortex	-53	-74	-14
			BA20	Inferior temporal gyrus	-54	-3	-37
			BA38	Temporopolar area	-46	19	-34
			BA47	Inferior frontal gyrus (pars orbitalis)	-50	35	-14
			BA6	SMA	9	25	63
					-6	25	63
			BA39	Angular gyrus	57	-59	40
			BA45	Inferior frontal gyrus (pars triangularis)	-50	25	-3
			BA46	Dorsolateral prefrontal cortex	49	42	1
			BA47	Inferior frontal gyrus (pars orbitalis)	57	32	-6
			BA37	Fusiform gyrus	-55	-67	-17
			BA20	Inferior temporal gyrus	62	-19	-29
					-52	-12	-41
332-388 ms			BA21	Middle temporal gyrus	69	-11	-18
					-56	-12	-29
			BA38	Temporopolar area	-52	16	-29
			BA47	Inferior frontal gyrus (pars orbitalis)	-53	34	-13
			BA1	Primary somatosensory cortex	-66	-20	21
			BA8	Frontal eye field	28	19	50
			BA10	Anterior prefrontal cortex	17	70	3
			BA18	Secondary visual cortex	30	-97	-15
			BA37	Fusiform gyrus	55	-65	-19
					-66	-52	-17
400-488 ms			BA38	Temporopolar area	-44	20	-34
			BA46	Dorsolateral prefrontal cortex	-49	44	-2
			BA9	Dorsolateral prefrontal cortex	8	52	41
			BA10	Anterior prefrontal cortex	-47	52	-2
			BA20	Inferior temporal gyrus	-49	2	-37
			BA21	Middle temporal gyrus	69	-9	-20
			BA38	Temporopolar area	-47	19	-33
490-540 ms			BA46	Dorsolateral prefrontal cortex	-52	43	0
			BA47	Inferior frontal gyrus (pars orbitalis)	-47	36	-18
			BA1	Primary somatosensory cortex	-67	-16	20
			BA10	Anterior prefrontal cortex	-46	52	3
			BA20	Inferior temporal gyrus	62	-19	-29
					-56	-9	-30
			BA21	Middle temporal gyrus	70	-13	-17
			BA37	Fusiform gyrus	-63	-58	-22
			BA38	Temporopolar area	-51	18	-30
			BA40	Supramarginal gyrus	-66	-22	21
			BA47	Inferior frontal gyrus (pars orbitalis)	-50	33	-16

(continued on next page)

Table 4 – (continued)

		BA7	Superior parietal lobule	-14	-54	71
		BA10	Anterior prefrontal cortex	35	52	26
		BA18	Secondary visual cortex	-39	-94	2
		BA9	Dorsolateral prefrontal cortex	9	59	31
	490-884 ms			-4	59	32
552-688 ms		BA5	Superior parietal lobule	8	-43	80
		BA8	Frontal eye field	9	36	57
		BA10	Anterior prefrontal cortex	-33	53	-6
		BA19	Associative visual cortex	-51	-75	-14
				32	-90	-14
		BA20	Inferior temporal gyrus	-50	2	-37
		BA21	Middle temporal gyrus	70	-15	-16
		BA22	Superior temporal gyrus	68	-14	-9
		BA38	Temporopolar pole	-50	18	-31
		BA39	Angular gyrus	-62	-48	35
			Angular gyrus (superior part)	-61	-49	37
		BA47	Inferior frontal gyrus (pars orbitalis)	-51	33	-14
		BA18	Secondary visual cortex	31	-96	-16
		BA10	Anterior prefrontal cortex	31	-57	-3
		BA20	Inferior temporal gyrus	54	-12	-40
780-1000 ms		BA7	Superior parietal lobule	-22	-65	70
		BA18	Secondary visual cortex	-41	-92	3
		BA19	Associative visual cortex	-51	-81	3
		BA9	Dorsolateral prefrontal cortex	-26	47	38
		BA10	Anterior prefrontal cortex	-18	62	-7
		BA39	Angular gyrus (superior part)	-60	-47	38
		BA9	Dorsolateral prefrontal cortex	9	57	32
				-2	57	34
		BA45	Inferior frontal gyrus (pars triangularis)	-57	25	3
		BA9	Dorsolateral prefrontal cortex	9	57	32
	984-1000 ms					
		BA45	Inferior frontal gyrus (pars triangularis)	-57	25	3

Local maxima are in MNI coordinates. The maxima with an amplitude greater than 70% are indicated in bold, while the local maxima with an amplitude greater than 51% (with a minimum size of 10) are provided in light grey in the table. Common microstate time periods are highlighted in dark grey. Microstate time periods specific to social stimuli are highlighted in dark blue, while microstate time periods specific to non-social stimuli are highlighted in aqua blue.

Fig. 4 and are summarized in **Table 5**. Brain source localization estimates showed the first microstate across Word Type shared involvement of the extrastriate and fusiform cortex, but the positive social words also elicited an early involvement of the precuneus. The second, long microstate elicited by nonsocial words appeared to focus on response preparation, whereas the three discrete microstates evoked by positive social words over the same time period in the Stroop task again reflected activation in a much more distributed set of brain regions including those involved in orienting and executive control aspects of attention and in social cognition (**Table 5**).

The second simple effects test focused the contrast between Positive Social and Nonsocial Words in subjects low in loneliness. The contrast indicated that the first two microstates (from 144 to 172 msec and from 188 to 200 msec) were the same for positive social and positive nonsocial words, with source estimates again suggesting the involvement in sensory cortical regions commonly found in fMRI studies of the Stroop task (i.e., the secondary visual cortex and associative visual cortex within the extrastriate cortex). Then, our results revealed significant differences in the two ERP waveforms as a function of Word Type for the periods ranging from 200 to 594 msec and from 632 to 1000 msec. The positive nonsocial words elicited an additional three microstates, whereas the positive social words elicited an additional five microstates that tended to be shorter in duration and differed in configuration. Accordingly, the microstate structure prior to 200 msec

and between 596 and 630 msec was defined based on analyses of the ERP collapsed across Word Type within subjects low in loneliness, and the microstate structure for the periods ranging from 200 to 594 msec and from 632 to 1000 msec identified in analyses of the ERP within Word Type for subjects low in loneliness. The statistically significant results ($p < .05$) of this analysis are depicted in the top panel of **Fig. 5**.

The estimated distributed cortical sources for these evoked microstates are illustrated in the bottom panel of **Fig. 5** and are summarized in **Table 6**.

Brain source localization estimates of these microstates suggested that both nonsocial and social positive words evoked the recruitment of similar brain regions sustaining functions such as pleasant stimuli processing, theory of mind, visual attention, orienting, executive control, and attention, but in different combinations and temporal sequences.

4. Discussion

Our focus here was on the effects of stimulus conditions and loneliness on microstate structure and timing to test our hypothesis and on the use source localization estimates to generate hypotheses regarding the underlying neural mechanisms for these microstates. Prior behavioral theory and research suggested that individuals high, in contrast to low, in loneliness are characterized by an implicit hyper-vigilance for social threats (Cacioppo et al., 2006; Cacioppo,

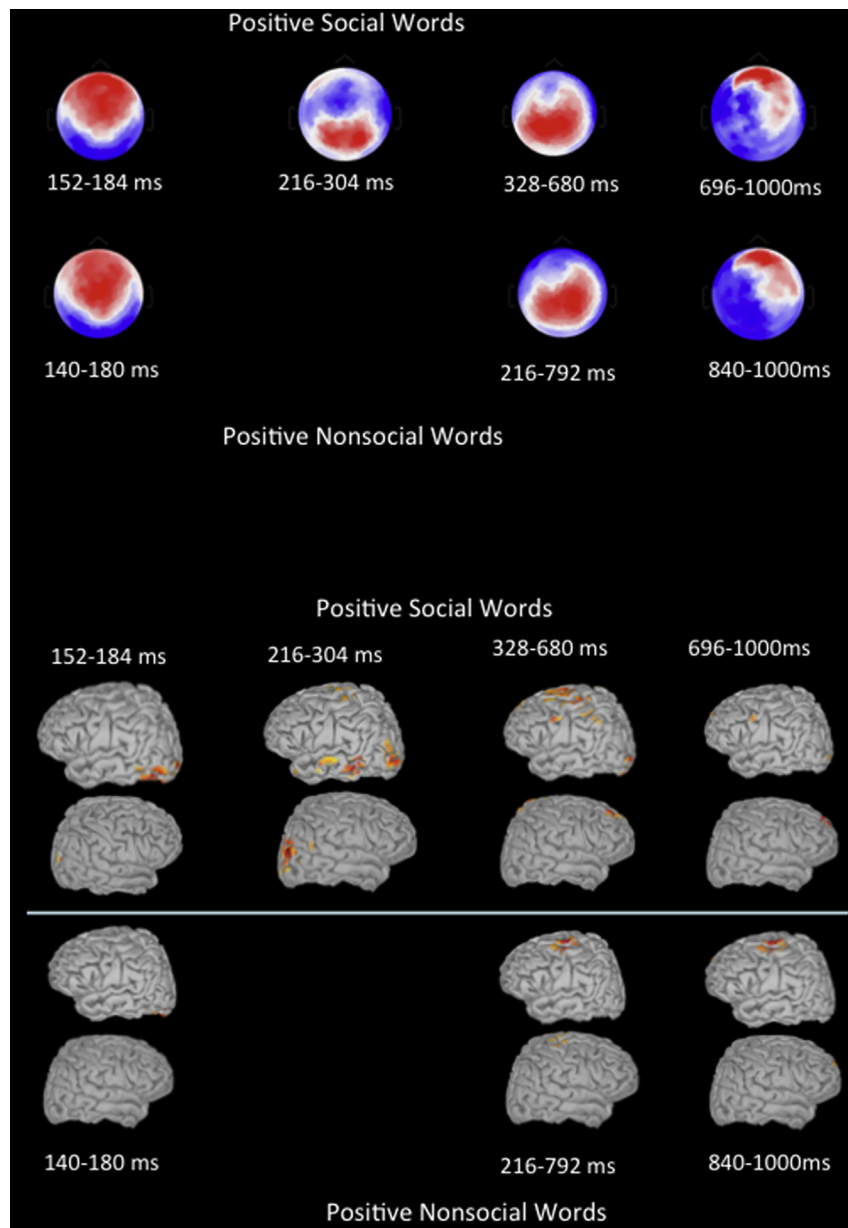


Fig. 4 – Brain microstates evoked in individuals high in loneliness in response to positive social and nonsocial words in the Stroop task. Top panel: Template maps for each discrete microstate. Bottom panel: Cortical source estimations were calculated for each discrete microstate.

Cacioppo, et al., 2015; Cacioppo, Grippo, London, Goossens, & Cacioppo, 2015). We used a social Stroop task and a new quantitative approach (CENA; Cacioppo, Weiss, et al., 2014) for analyzing high-density ERP waveforms over a 128-sensor space to test the experimental hypothesis that the implicit attention to negative social (in contrast to nonsocial) stimuli differs between individuals high versus low in loneliness. The Loneliness (high, low) \times Word Type (social, nonsocial) interaction for the negative words in the Stroop task indicated the microstates elicited in lonely and nonlonely subjects differed significantly as a function of Word Type beginning as early as 280 msec following stimulus onset. In

accord with the previous behavioral differences suggesting lonely individuals are predisposed to orient to negative social stimuli, the differentiation of negative social from negative nonsocial words by brain microstates evoked in the Stroop task occurred approximately 200 msec earlier in individuals high in loneliness than in individuals low in loneliness.

The interaction test and simple main effects test within lonely subjects showed that the first three microstates elicited by negative words in the Stroop task, which appeared within the first 280 msec, did not differ for negative social and nonsocial words. Although exploratory, inspection of the source localization of each one of these three microstates

Table 5 – Local maxima of current source density obtained from wMNE brain source estimations for High lonely in response to Social Positive Stimuli (in dark blue) versus Non-Social Positive Stimuli (in aqua blue).

Microstate time periods for Social Positive	Microstate time periods for Non-Social Positive	Brodmann Areas	Brain region labels	MNI Brain coordinates		
				x	y	z
152-184 ms			BA7 Superior parietal lobule	35	-61	58
			BA18 Secondary visual cortex	35	-97	7
				-36	-87	12
			BA19 Associative visual cortex	-48	-82	-2
				35	-90	25
			BA37 Fusiform gyrus	-58	-67	-16
			BA10 Anterior prefrontal cortex	33	56	6
			BA39 Angular gyrus	-63	-53	10
			BA18 Secondary visual cortex	-31	-95	-18
			BA19 Associative visual cortex	-42	-84	-14
216-304 ms			BA37 Fusiform gyrus	-49	-77	-15
			BA39 Angular gyrus (superior part)	-36	-70	49
			BA1 Primary somatosensory cortex	-39	-33	62
			BA6 SMA	-22	-12	76
			BA7 Superior parietal lobule	-39	-46	59
			BA18 Secondary visual cortex	-35	-91	-8
			BA19 Associative visual cortex	40	-87	26
			BA21 Middle temporal gyrus	-70	-22	-4
			BA37 Fusiform gyrus	-68	-54	-8
			BA39 Angular gyrus	53	-61	26
			BA38 Temporopolar pole	-51	17	-33
			BA39 Angular gyrus	-57	-55	31
			BA45 Inferior frontal gyrus (pars triangularis)	-51	28	-1
			BA46 Dorsolateral frontal gyrus	49	39	6
328-680 ms			BA47 Inferior frontal gyrus (pars orbitalis)	-51	27	-4
			BA6 SMA	43	-19	65
				-39	-8	63
			BA1 Primary somatosensory cortex	-38	-33	64
			BA19 Associative visual cortex	43	-82	31
			BA1 Primary somatosensory cortex	-45	-23	58
			BA6 SMA	12	-33	75
			BA7 Superior parietal lobule	26	-74	55
			BA9 Dorsolateral prefrontal cortex	-29	43	35
			BA18 Secondary visual cortex	-25	-103	6
696-1000 ms			BA19 Associative visual cortex	47	-76	28
			BA10 Anterior prefrontal cortex	-10	66	25
			BA37 Fusiform gyrus	-60	-60	23
			BA39 Angular gyrus	42	-81	32
				-52	-59	48
			BA6 SMA	-60	5	38
			BA9 Dorsolateral prefrontal cortex	17	59	30
			BA10 Anterior prefrontal cortex	-14	62	25
				16	62	25
			BA18 Secondary visual cortex	-25	-103	4
840-1000 ms			BA4 Primary motor cortex	-60	-9	38
			BA44 Inferior frontal cortex (pars opercularis)	-51	20	30
			BA39 Angular gyrus	-53	-53	50
			BA6 SMA	-40	-6	63
			BA8 Frontal eye field	17	29	58
			BA10 Anterior prefrontal cortex	17	65	18
			BA6 SMA	20	-18	77

Local maxima are in MNI coordinates. The maxima with an amplitude greater than 70% are indicated in bold, while the local maxima with an amplitude greater than 51% (with a minimum size of 10) are provided in light grey in the table. Common microstate time periods are highlighted in dark grey. Microstate time periods specific to social stimuli are highlighted in dark blue, while microstate time periods specific to non-social stimuli are highlighted in aqua blue.

within the first 280 msec revealed a pattern of activation within brain areas known to sustain visual attention (extrastriate cortex; Corbetta, Miezin, Dobmeyer, Shulman, & Petersen, 1990; Polk, Drake, Jonides, Smith, & Smith, 2008), visual word processing (fusiform gyrus; e.g., McCandliss, Cohen, & Dehaene, 2003), as well as response conflict in a Stroop task (e.g., anterior cingulate cortex, precuneus; Bench et al., 1993; Banich et al., 2000; Polk et al., 2008).

Next, after 280 msec post-stimulus, differential brain sources estimations were observed between negative social and negative nonsocial stimuli. Comparison of source localization estimates for these microstates raised the hypothesis that the negative social, in contrast to nonsocial, words in the Stroop task elicited activation in more brain regions involved

in the orienting and executive control aspects of visual attention—an early brain pattern in line with the evolutionary hypothesis that loneliness is associated with an implicit hyper-attention to negative social stimuli as they are perceived as potential social threats (Bangee et al., 2014; Qualter et al., 2013; Cacioppo, Cacioppo, et al., 2015; Cacioppo, Grippo, et al., 2015 for review). According to the evolutionary model of loneliness, feeling socially isolated (or on the social perimeter) leads to increased surveillance of the social world and an unwitting focus on self-preservation (Cacioppo et al., 2006; Cacioppo, Capitanio, et al., 2014; Cacioppo, Weiss, et al., 2014; Cacioppo, Cacioppo, et al., 2015; Cacioppo, Grippo, et al., 2015). This distinction was not observed in subjects low in loneliness (Table 4).

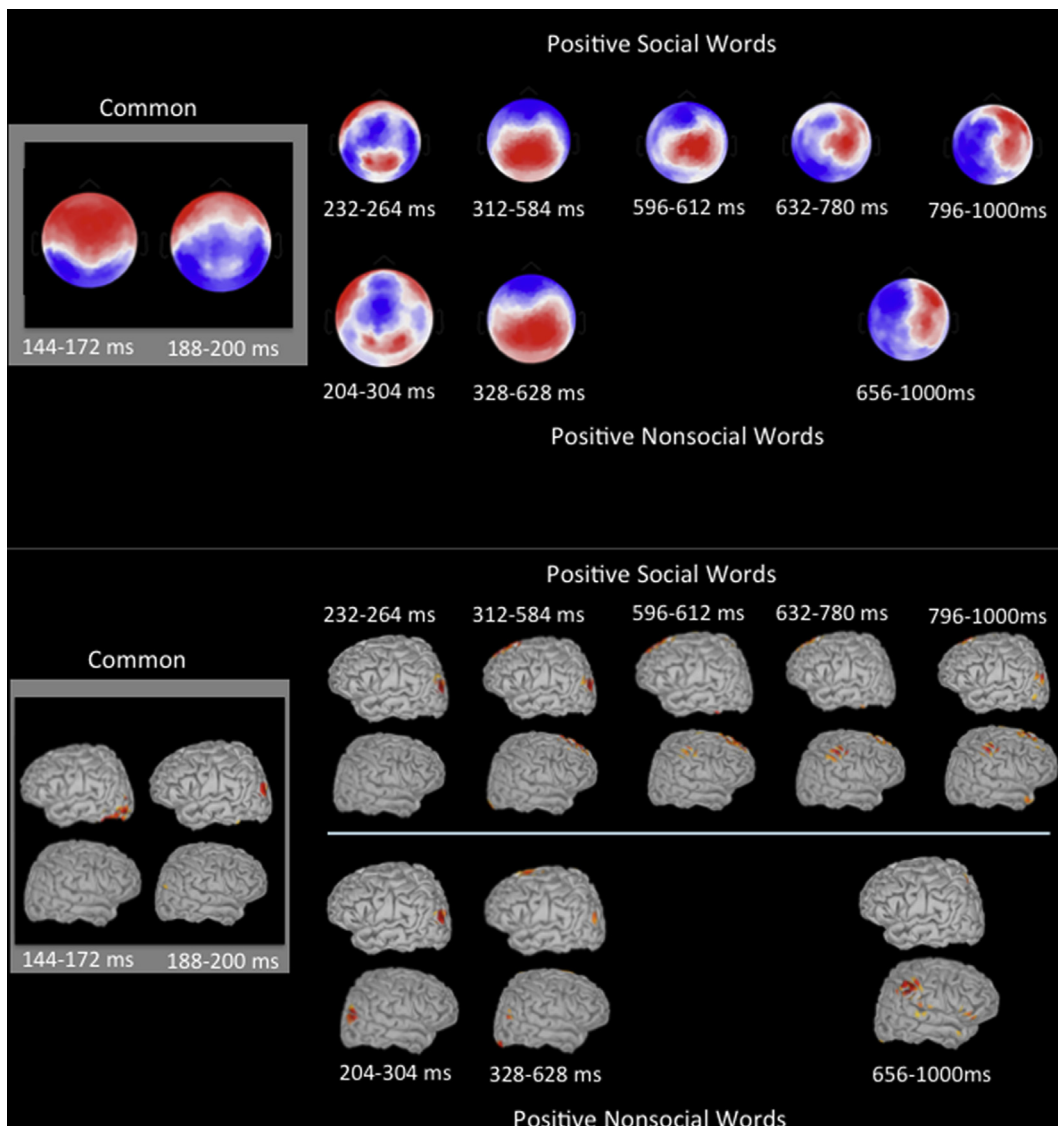


Fig. 5 – Brain microstates evoked in individuals low in loneliness in response to positive social and nonsocial words in the Stroop task. Top panel: Template maps for each discrete microstate. Bottom panel: Cortical source estimations were calculated for each discrete microstate.

To put the present results in context, it is noteworthy that the distribution of loneliness in the population is negatively skewed, with most people characterized by low levels of loneliness (Cacioppo & Patrick, 2008). The results from nonlonely subjects, therefore, would be expected to be more similar to the results one would find when individual differences are not considered. In line with this, the simple main effects test within nonlonely subjects indicated that the first five microstates elicited by the Stroop task were the same for negative social and negative nonsocial words, and source estimates of these early microstates suggested the involvement in neural regions commonly found in fMRI studies of the Stroop task. The evoked brain microstates in nonlonely subjects that emerged approximately 490 msec following stimulus onset were different for negative social and nonsocial words, and each of these microstates was followed

by two late microstates that also differed as a function of word type.

In terms of positive words processing, the interaction test and simple main effects test within lonely subjects revealed that all of the microstates elicited by positive social and nonsocial words differed as a function of word type (see Fig. 4). The first microstate evoked by positive words in the Stroop task began later than the first microstate evoked by negative words, as might be expected from the prior behavioral research on the emotional Stroop task (Williams, Mathews, & MacLeod, 1996). Interestingly, the Loneliness × Word Type interaction indicated the microstates elicited by positive words in lonely and nonlonely subjects differed significantly for positive social and nonsocial stimuli beginning as early as 136 msec following stimulus onset and considerably earlier than Word Type influenced the microstates elicited by

Table 6 – Local maxima of current source density obtained from wMNE brain source estimations for Low lonely in response to Social Positive Stimuli (in dark blue) versus Non-Social Positive Stimuli (in aqua blue).

Microstate time periods for Social Positive	Microstate time periods for Non-Social Positive	Brodmann Areas	Brain region labels	MNI Brain coordinates			
				x	y	z	
144-172 ms			BA18	Secondary visual cortex	-39	-94	-4
			BA19	Associative visual cortex	-52	-75	-14
			BA37	Fusiform gyrus	-62	-55	-14
			BA21	Middle temporal gyrus	-59	-26	-19
188-200 ms			BA19	Associative visual cortex	-36	-88	28
			BA21	Middle temporal gyrus	-61	-26	-17
			BA37	Fusiform gyrus	-61	-61	-21
			BA39	Angular gyrus	44	-80	33
232-264 ms			BA19	Associative visual cortex	-36	-88	28
					42	-85	25
204-304 ms			BA8	Frontal eye field	7	33	58
			BA19	Associative visual cortex	43	-84	25
					-37	-86	31
			BA39	Angular gyrus	46	-78	31
					-28	-81	40
			BA6	SMA	-18	16	64
			BA10	Anterior prefrontal cortex	-47	42	22
			BA8	Frontal eye field	-8	30	60
312-584 ms					24	30	43
			BA9	Dorsolateral prefrontal cortex	9	51	43
			BA19	Associative visual cortex	-27	-91	28
			BA6	SMA	54	-10	52
					-8	-9	69
			BA18	Secondary visual cortex	20	-104	-9
			BA39	Angular gyrus	-52	-66	30
			BA32	Dorsal anterior cingulate cortex	-5	37	26
328-628 ms			BA8	Frontal eye field	28	21	50
			BA9	Dorsolateral prefrontal cortex	28	40	39
			BA18	Secondary visual cortex	30	-98	-14
			BA19	Associative visual cortex	50	-76	26
			BA6	SMA	-7	25	64
					8	22	64
596-612 ms			BA39	Angular gyrus	59	-60	29
			BA1	Primary somatosensory cortex	53	-17	49
			BA7	Superior parietal lobule	-21	-58	73
			BA9	Dorsolateral prefrontal cortex	-4	54	40
					24	49	28
			BA37	Fusiform gyrus	-63	-58	-23
			BA6	SMA	14	-3	76
					-6	-3	74
			BA10	Anterior prefrontal cortex	33	56	7
			BA18	Secondary visual cortex	26	-102	7
632-780 ms			BA32	Dorsal anterior cingulate cortex	-5	37	25
			BA40	Supramarginal gyrus	61	-29	47
			BA1	Primary somatosensory cortex	47	-28	61
			BA8	Frontal eye field	12	43	48
			BA9	Dorsolateral prefrontal cortex	26	47	32
			BA40	Supramarginal gyrus	61	-28	47
796-1000 ms			BA8	Frontal eye field	-11	42	53
			BA10	Anterior prefrontal cortex	32	51	20
			BA22	Superior posterior temporal gyrus	62	-36	22
			BA37	Fusiform gyrus	-64	-57	-22
			BA1	Primary somatosensory cortex	55	-24	54
			BA6	SMA	47	-18	61
			BA8	Frontal eye field	10	38	55
			BA9	Dorsolateral prefrontal cortex	27	38	41
			BA19	Associative visual cortex	-37	-86	31

Table 6 – (continued)

		BA38 BA39 BA6 BA8 BA18 BA32	Temporopolar pole Angular gyrus SMA Frontal eye field Secondary visual cortex Dorsal anterior cingulate cortex	54 -47 -9 -8 -44 -6	15 -77 -4 34 -89 34	-36 34 74 57 -2 29
	656–1000 ms	BA18 BA38 BA39 BA40 BA47 BA7 BA10 BA13 BA44	Secondary visual cortex Temporopolar pole Angular gyrus Supramarginal gyrus Inferior frontal gyrus (pars orbitalis) Superior parietal lobule Anterior prefrontal cortex Anterior Insula Inferior frontal gyrus (pars opercularis)	27 55 56 59 47 -13 0 44 44	-99 15 -55 50 -16 -79 60 18 15	-15 -34 45 50 -16 57 13 -10 13

Local maxima are in MNI coordinates. The maxima with an amplitude greater than 70% are indicated in bold, while the local maxima with an amplitude greater than 51% (with a minimum size of 10) are provided in light grey in the table. Common microstate time periods are highlighted in dark grey. Microstate time periods specific to social stimuli are highlighted in dark blue, while microstate time periods specific to non-social stimuli are highlighted in aqua blue.

negative words in the Stroop task. These results suggest that although negative stimuli may elicit attention more quickly, the early processing of negative stimuli may be less nuanced – or at least less sensitive to social characteristics of the stimuli – than the early processing of positive stimuli.

The simple main effects test within *non-lonely* subjects indicated that the first two microstates elicited by the Stroop task were the same for positive social and positive nonsocial words, with source estimates within visual cortical regions commonly found in fMRI studies of the Stroop task. The positive nonsocial words elicited an additional three microstates, whereas the positive social words elicited an additional five microstates that tended to be shorter in duration and differed in configuration. In sum, the differences in the microstate structure between individuals high and low in loneliness are in line with differences in social threat surveillance the evolutionary model of loneliness predicted (Cacioppo & Hawkley, 2009; Cacioppo, Cacioppo, et al., 2015; Cacioppo, Grippo, et al., 2015 for review). Indeed, the present study provides the first evidence that negative social stimuli are differentiated from negative nonsocial stimuli more quickly in the lonely than nonlonely brains. Given the timing of this differentiation in the brain and the fact that participants were performing a Stroop task, these results also suggest that these data reflect implicit rather than explicit attentional differences between lonely and nonlonely individuals.

In sum, the microstate timing and structure results are in accord with the evolutionary model of loneliness. A limitation of the present study is that it included a block design with a positive block systematically occurring after the practice block. Although we chose to randomize task order once and keep it constant across all subjects in order to improve our ability to detect individual differences in response to the tasks, a replication with an event-related design will increase our confidence in the generalizability of these findings. In addition, the exploratory sources estimates suggested that both orienting and executive control aspects of attention contribute to the differences we observed between lonely and nonlonely individuals. These hypotheses warrant further study investigation.

Acknowledgments

The authors thank Aaron B. Ball, Adina Bianchi, and Jasmin Cloutier for their technical assistance. Support for this research was provided by a grant awarded to JTC by the Department of the Army Award #W81XWH-11-2-0114.

Supplementary data

Supplementary data related to this article can be found at <http://dx.doi.org/10.1016/j.cortex.2015.05.032>.

REFERENCES

- Adam, E. K., Hawkley, L. C., Kudielka, B. M., & Cacioppo, J. T. (2006). Day-to-day dynamics of experience-cortisol associations in a population-based sample of older adults. *Proceedings of the National Academy of Sciences*, 103, 17058–17063.
- Baillet, S., Mosher, J. C., & Leahy, R. M. (2001). Electromagnetic brain mapping. *Signal Processing Magazine, IEEE*, 18, 14–30. <http://dx.doi.org/10.1109/79.962275>.
- Banjee, M., Harris, R. A., Bridges, N., Rotenberg, K. J., & Qualter, P. (2014). Loneliness and attention to social threat in young adults: findings from an eye tracker study. *Personality and Individual Differences*, 63, 16–23.
- Banich, M. T., Milham, M. P., Atchley, R., Cohen, N. J., Webb, A., Wszalek, T., et al. (2000). fMRI studies of Stroop tasks reveal unique roles of anterior and posterior brain systems in attentional selection. *Journal of Cognitive Neuroscience*, 12, 988–1000.
- Bench, C. J., Frith, C. D., Grasby, P. M., Friston, K. J., Paulesu, E., Frackowiak, R. S., et al. (1993). Investigations of the functional anatomy of attention using the Stroop test. *Neuropsychologia*, 31, 907–922.
- Bradley, M. M., & Lang, P. J. (1999). *Affective norms for English words (ANEW): Instruction manual and affective ratings* (Tech. Rep. No. C-1). Gainesville, FL: University of Florida, The Center for Research in Psychophysiology.
- Button, K. S., Ioannidis, J. P., Mokrysz, C., Nosek, B. A., Flint, J., Robinson, E. S., et al. (2013). Power failure: why small sample

- size undermines the reliability of neuroscience. *Nature Reviews Neuroscience*, 14, 365–376.
- Cacioppo, J. T., Cacioppo, S., Capitanio, J. P., & Cole, W. W. (2015). The neuroendocrinology of social isolation. *Annual Review of Psychology*, 66, 9.1–9.35.
- Cacioppo, J. T., Fowler, J. H., & Christakis, N. A. (2009). Alone in the crowd: the structure and spread of loneliness in a large social network. *Journal of Personality and Social Psychology*, 97, 977–991.
- Cacioppo, S., Frum, C., Asp, E., Weiss, R. M., Lewis, J. W., & Cacioppo, J. T. (2013). A quantitative meta-analysis of functional imaging studies of social rejection. *Scientific Reports*, *Nature Journal*, 3, 2027. <http://dx.doi.org/10.1038/srep02027>.
- Cacioppo, S., Grippo, A. J., London, S., Goossens, L., & Cacioppo, J. T. (2015). Loneliness: clinical import and interventions. *Perspectives on Psychological Science*, 10, 238–249.
- Cacioppo, J. T., & Hawkley, L. C. (2009). Perceived social isolation and cognition. *Trends in Cognitive Science*, 13, 447–454. <http://dx.doi.org/10.1016/j.tics.2009.06.005>.
- Cacioppo, J. T., Hawkley, L. C., Ernst, J. M., Burleson, M., Berntson, G. G., Nouriani, B., et al. (2006). Loneliness within a nomological net: an evolutionary perspective. *Journal of Research in Personality*, 40, 1054–1085.
- Cacioppo, J. T., Hawkley, L. C., & Thisted, R. A. (2010). Perceived social isolation makes me sad: five year cross-lagged analyses of loneliness and depressive symptomatology in the Chicago Health, Aging, and Social Relations Study. *Psychology and Aging*, 25, 453–463.
- Cacioppo, J. T., Norris, C. J., Decety, J., Monteleone, G., & Nusbaum, H. (2009). In the eye of the beholder: Individual differences in perceived social isolation predict regional brain activation to social stimuli. *Journal of Cognitive Neuroscience*, 21, 83–92.
- Cacioppo, J. T., & Patrick, B. (2008). *Loneliness: Human nature and the need for social connection*. New York: W. W. Norton & Company.
- Cacioppo, S., Bianchi-Demicheli, F., Bischof, P., DeZiegler, D., Michel, C. M., & Landis. (2013). Hemispheric specialization varies with EEG brain resting states and phase of menstrual cycle. *PLoS One*, 8, e63196.
- Cacioppo, S., Capitanio, J. P., & Cacioppo, J. T. (2014). Toward a neurology of loneliness. *Psychological Bulletin*, 140, 1464–1504.
- Cacioppo, S., Weiss, R. M., Runesha, H. B., & Cacioppo, J. T. (2014). Dynamic spatiotemporal brain analyses using high performance electrical neuroimaging: theoretical framework and validation. *Journal of Neuroscience Methods*, 238, 11–34.
- Capitanio, J. P., Hawkley, L. C., Cole, S. W., & Cacioppo, J. T. (2014). A behavioral taxonomy of loneliness in monkeys and humans. *PLoS One*, 9, e110307. <http://dx.doi.org/10.1371/journal.pone.0110307>.
- Collins, D. L., Zijdenbos, A. P., Kollokian, V., Sled, J. G., Kabani, N. J., Holmes, C. J., et al. (1998). Design and construction of a realistic digital brain phantom. *IEEE Transactions on Medical Imaging*, 17(3), 463–468. <http://dx.doi.org/10.1109/42.712135>.
- Corbetta, M., Miezin, F. M., Dobmeyer, S., Shulman, G. L., & Petersen, S. E. (1990). Attentional modulation of neural processing of shape, color, and velocity in humans. *Science*, 248, 1556–1559.
- Decety, J., & Cacioppo, S. (2012). The speed of morality: a high-density electrical neuroimaging study. *Journal of Neurophysiology*, 108, 3068–3072.
- Egidi, G., Shintel, H., Nusbaum, H. C., & Cacioppo, J. T. (2008). Social isolation and neural correlates of attention control. In *20th Annual Meeting of the Association for Psychological science; Chicago, IL*.
- Fox, M. W. (1967). The effects of short-term social and sensory isolation upon behavior, EEG, and averaged evoked potential in puppies. *Physiology and Behavior*, 2, 145–151.
- Gable, S. (2006). Approach and avoidance social motives and goals. *Journal of Personality*, 74, 175–222.
- Gemignani, A., Piarulli, A., Menicucci, D., Laurino, M., Rota, G., Mastorci, F., et al. (2014). How stressful are 105 days of isolation? Sleep EEG pattern and tonic cortisol in healthy. *International Journal of Psychophysiology*, 93, 211–219.
- Gramfort, A., Papadopoulou, T., Olivi, E., & Clerc, M. (2010). OpenMEEG: opensource software for quasistatic bioelectromagnetics. *Biomedical Engineering Online*, 9, 45. <http://dx.doi.org/10.1186/1475-925X-9-45>.
- Grippo, A., Ihm, E., Wardwell, J., McNeal, N., Scotti, M., Moenk, D. A., et al. (2014). The effects of environmental enrichment on depressive and anxiety-relevant behaviors in socially isolated prairie voles. *Psychosomatic Medicine*, 76, 277–284.
- Heikkinen, R. L., & Kauppinen, M. (2004). Depressive symptoms in late life: a 10-year follow-up. *Archives of Gerontology and Geriatrics*, 38, 239–250.
- Ioannou, C. C., Guttal, V., & Couzin, I. D. (2012). Predatory fish select for coordinated collective motion in virtual prey. *Science*, 337, 1212–1215.
- Khanna, A., Pascual-Leone, A., Michel, C. M., & Farzan, F. (2015). Microstates in resting-state EEG: current status and future directions. *Neuroscience and Biobehavioral Reviews*, 49, 105–113.
- Kucera, H., & Francis, W. N. (1967). *Computational analysis of present-day American English*. Providence, RI: Brown University Press.
- Kurina, L. M., Knutson, K. L., Hawkley, L. C., Cacioppo, J. T., Lauderdale, D. S., & Ober, C. (2011). Loneliness is associated with sleep fragmentation in a communal society. *Sleep*, 34, 1519–1526.
- Kybic, J., Clerc, M., Abboud, T., Faugeras, O., Keriven, R., & Papadopoulou, T. (2005). A common formalism for the integral formulations of the forward EEG problem. *Medical Imaging, IEEE Transactions on*, 24, 12–28. <http://dx.doi.org/10.1109/tmi.2004.837363>.
- Lehmann, D. (1987). Principles of spatial analysis. In A. S. Gevins, & A. Re mond (Eds.), *Handbook of electroencephalography and clinical neurophysiology: Methods of analysis of brain electrical and magnetic signals* (pp. 309–354). Amsterdam: Elsevier.
- Lehmann, D., & Skrandies, W. (1980). Reference-free identification of components of checkerboard-evoked multichannel potential fields. *Electroencephalography Clinical Neurophysiology*, 48, 609–621.
- McCandiss, B. D., Cohen, L., & Dehaene, S. (2003). The visual word form area: expertise for reading in the fusiform gyrus. *Trends in Cognitive Sciences*, 7, 293–299.
- Michel, C. M., Seeck, M., & Landis, T. (1999). Spatiotemporal dynamics of human cognition. *News in Physiological Sciences*, 14, 206–214.
- Oldfield, R. C. (1971). The assessment and analysis of handedness: the Edinburgh inventory. *Neuropsychologia*, 9, 97–113.
- Ortigue, S., Siniaglia, C., Rizzolatti, G., & Grafton, S. T. (2010). Understanding actions of others: the electrodynamics of the left and right hemispheres. A high-density EEG neuroimaging study. *PLoS One*, 5, e12160.
- Pascual-Marqui, R. D., Michel, C. M., & Lehmann, D. (1995). Segmentation of brain electrical activity into microstates: model estimation and validation. *IEEE Transactions on Biomedical Engineering*, 42, 658–665.
- Perrin, F., Pernier, J., Bertrand, O., Giard, M. H., & Echallier, J. F. (1987). Mapping of scalp potentials by surface spline interpolation. *Electroencephalography and Clinical Neurophysiology*, 66, 75–81.

- Polk, T. A., Drake, R. M., Jonides, J. J., Smith, M. R., & Smith, E. E. (2008). Attention enhances the neural processing of relevant features and suppresses the processing of irrelevant features in humans: an fMRI study of the Stroop task. *Journal of Neuroscience*, 28, 13786–13792.
- Qualter, P., Rotenberg, K. J., Barrett, L., Henzi, P., Barlow, A., Stylianou, M. S., et al. (2013). Investigating hypervigilance for social threat of lonely children. *Journal of Abnormal Child Psychology*, 41, 325–338. <http://dx.doi.org/10.1007/s10802-012-9676-x>.
- Rasmussen, J. E. (1973). *Man in isolation & confinement*. Chicago: Aldine Pub. Co.
- Russell, D. (1996). UCLA Loneliness Scale (Version 3): reliability, validity, and factor structure. *Journal of Personality Assessment*, 66, 20–40.
- Tadel, F., Baillet, S., Mosher, J. C., Pantazis, D., & Leahy, R. M. (2011). Brainstorm: a user-friendly application for MEG/EEG analysis. *Computational Intelligence and Neuroscience*, 2011, 13. <http://dx.doi.org/10.1155/2011/879716>. Article ID 879716.
- Tzourio-Mazoyer, N., Landeau, B., Papathanassiou, D., Crivello, F., Etard, O., Delcroix, N., et al. (2002). Automated anatomical labeling of activations in SPM using a macroscopic anatomical parcellation of the MNI MRI single-subject brain. *NeuroImage*, 15, 273–289. <http://dx.doi.org/10.1006/nimg.2001.0978>.
- VanderWeele, T. J., Hawkley, L. C., Thisted, R. A., & Cacioppo, J. T. (2011). A marginal structural model analysis for loneliness: implications for intervention trials and clinical practice. *Journal of Clinical and Consulting Psychology*, 79, 225–235.
- Williams, J. M. G., Mathews, A., & MacLeod, C. (1996). The emotional Stroop task and psychopathology. *Psychological Bulletin*, 120, 3–24.
- Wilson, R. S., Krueger, K. R., Arnold, S. E., Schneider, J. a, Kelly, J. F., Barnes, L. L., et al. (2007). Loneliness and risk of Alzheimer disease. *Archives of General Psychiatry*, 64, 234–240.
- Yamada, M., & Decety, J. (2009). Unconscious affective processing and empathy: an investigation of subliminal priming on the detection of painful facial expressions. *Pain*, 143, 71–75.
- Zigmond, A. S., & Snaith, R. P. (1983). The hospital anxiety and depression scale. *Acta Psychiatrica Scandinavica*, 67, 361–370.
- Zubek, J. P., Bayer, L., & Shepard, J. M. (1967). Relative effects of prolonged social isolation and confinement: behavioral and EEG changes. *Journal of Abnormal Psychology*, 74, 625–631.